Desalination and Water Treatment
www.deswater.com

doi: 10.5004/dwt.2017.20269

65 (2017) 233–242
February

Decolorization of eosin-Y dye using activated carbon electrode prepared from bael fruit (*Aegle marmelos*) shell

N. Mohanraj, S. Bhuvaneshwari*

Department of Chemical Engineering, National Institute of Technology Calicut, Kozhikode 673601, Kerala, India, Tel. +91-4952285402; email: sbuvana@nitc.ac.in (S. Bhuvaneshwari), Tel. +91-9567780055; email: nmohanraj2006@gmail.com (N. Mohanraj)

Received 8 May 2016; Accepted 13 October 2016

ABSTRACT

In the present scenario, electrode materials used in electrochemical processes are moderately expensive; hence, low-cost electrode material obtains more importance. The current study examined the potential of electroadsorption of eosin-Y dye on activated carbon electrode (ACE) and carbon composite electrode (CCE) prepared from bael fruit (*Aegle marmelos*) shell (BS). This study holds the novelty of ACE prepared from BS carbon using H_3PO_4 activation, and also compositing technique was adopted to improve the conductivity of the ACE. In addition to good electrical conductivity, the electrode prepared is also cost-effective. The factors like applied potential, contact time and initial dye concentration were varied to obtain specific information about the influence of them on the adsorption ability and adsorption equilibrium. UV-visible spectrophotometric analysis method was used to find the capacity of eosin-Y dye color removal. Surface area and pore volume analysis were carried out using Brunauer-Emmett-Teller apparatus. The other characterization of the activated carbon, ACE and CCE were done using different analytical instruments like scanning electron microscope for surface morphology, energy-dispersive X-ray spectroscopy for elemental investigation and thermogravimetric analysis for thermal stability of BS adsorbent. The isotherm models as Langmuir, Freundlich and Jovanovic were used to analyze the equilibrium data of electrosorption. Freundlich isotherm was found to be the most suitable with a correlation coefficient ($R^2 = 0.923$). Kinetic studies were performed for pseudo-first-order, pseudo-second-order and intraparticle diffusion model. The experimental data were found to fit well with the pseudo-first-order kinetic model, with $R^2 = 0.969$. It has been observed that modifications in surface properties of electrode play a major role in dye wastewater treatment processes. The results showed that the CCE is best suitable for the application of dye color removal compared with ACE, using electrosorption techniques.

Keywords: Activated carbon; Eosin-Y dye; Electrode; Electrosorption

1. Introduction

Textile dyes are well-known mutagens and carcinogens posing risks to various ecosystems, animals' health and agriculture; therefore, the treatment of these high volumes of wastewater becomes crucial. The textile industries are using more than 8,000 chemicals in various processes of textile manufacturing, which include dyeing and printing. Azo dyes, reactive dyes and acidic dyes are the prime group of dyes used in the textile industries and contribute between 50% and 65% of the colors in textile dyes. Consequently, these dyes find their way to the environment and end up contaminating rivers and groundwater in the locale of the industries. Various types of dyes used in textile industries are very difficult to remove. Textile wastewater treatment includes numerous biological, physical and chemical methods, but these methods are cost-effective. The most efficient treatment methods are based on adsorption of contaminants onto activated carbon (AC), which appears to be the best method of removing dye due to its high surface area,

* Corresponding author.

porous nature and high adsorption capacity [1,2]. However, this process is expensive and difficult to regenerate after use. Therefore, technology need to be upgraded and/or replaced with new or more advanced water treatment processes that can provide high-quality treated water. In current scenario, electrosorption has been initiated as alternative technique. In line with the growing anxiety on the environment-friendly technologies and achieving the status of green industrial policy, a supportive engineering measure, electrosorption technique which incorporating electrochemical innovation in the adsorption science, has lately released extended interest all around the globe [3,4]. Electrosorption deals with an effect of applied electrical potential on the sorption behavior [5]. The selectivity of ions in electrosorption depends on the surface properties of the electrode and properties of the ions. The electrosorption combines the enhancement of adsorption rate and capacity by polarization and electrochemical regeneration. The potential of electrosorption techniques for wastewater treatment represents a potentially viable and powerful tool, leading to the superior improvement of pollution control and environmental preservation [6,7]. Several literature studies state that electrosorption processes using carbon materials as electrodes have succeeded in removing various unwanted ions or charged contaminants from aqueous solutions, brackish water and groundwater [8]. Studies have been carried out on electroadsorption for the removal of acilan blau dye from textile effluents by using commercial granular AC. In another research, electrochemical polarization to enhance adsorption rate and capacity of acid orange 7 dye using AC fiber was investigated. For effective removal of pollutants from electroplating, fertilizer, textile wastewater, paint and pigments in a low energy consumption, electrosorption treatment will be the right option due its simple experimental designs, low cost and high efficiency [9,10].

Hence, this study focused on developing activated carbon electrode (ACE) from non-usable bael fruit shell for the treatment of dye from wastewater and to improve the conductivity of electrodes by different feasible processes. Preparation of AC, ACE and carbon composite electrode (CCE) were discussed. The effects of time in the range of 15–150 min, initial dye concentration in the range of 25–200 mg L^{-1} and applied voltage in the range of 5–45 V on the removal efficiency of eosin-Y dye were studied and optimized [11,12]. The equilibrium data for the batch electroadsorption of eosin-Y dye were tested with Langmuir, Freundlich and Jovanovic isotherm models. The kinetics of electroadsorption were analyzed using the pseudo-first-order, pseudo-second-order and intraparticle models.

2. Materials and methods

2.1. Preparation of activated carbon

In this study, a new ACE prepared from a non-usable bael fruit (*Aegle marmelos*) shell (BS) was used. BS was washed with enough quantity of tap water to remove impurities and surface adhered particles. It was kept for drying in hot air oven at 110°C, granulated using pulverizer and sieved using sieve shaker for the range 0.25–0.5 mm using the mesh 60–35. Chemical activation of BS was done by acid and alkalis like HCl, H_2SO_4, KOH, NaCl, NaOH and H_3PO_4. Based on the result, H_3PO_4 activation was chosen for further studies. Comparison efficiency of different adsorbents prepared with phosphoric acid activation by various researchers were listed in Table 1. Chemical activation of BS was carried out using 88% orthophosphoric acid in 1:1 weight ratio (bael shell:acid) and kept it for drying in hot air oven at 110°C for 2–3 h. The dried materials were heated to high temperature by using muffle furnace from room temperature to 600°C for the period of 90 min and immersed in 2% $NaHCO_3$ to detach the residual acid, which presents on the adsorbent, and washed several times with distilled water to remove the impurities on the surface of the adsorbent. Then the adsorbent was kept for drying at 110°C for 2 h and finally cooled in desiccator to remove the moisture content. The prepared AC was stored in the airtight container [13,14].

2.2. Development of activated carbon electrode

The prepared AC powder and poly(vinylidene fluoride) (PVDF; molecular weight = 534,000; Sigma-Aldrich product, Bengaluru, India) were used to prepare ACEs. 0.9 g of AC and 0.1 g of PVDF polymer were mixed with 1.5 mL of *N*,*N*-dimethylacetamide (DMAc, 99%) solvent to form a carbon slurry (CS) [20,21]. Then, the CS was made to an electrode of dimension 45 mm length, 15 mm width and 3 mm thickness, which weighed about 1.7 g. The prepared electrode was kept in a hot air oven for drying at 120°C for 2 h. Moreover, PVDF-bonded ACE were treated with 1 M KOH solution at normal room temperature for 24 h to improve the deionization efficiency. Finally, the ACE was cleaned with deionized water and dried in an oven at 70°C for 2 h [21,22].

2.3. Development of carbon composite electrode

A copper stick of 50 mm length and 2 mm width was placed at the center of CS and then kept in a hot air oven for drying at 120°C for 2 h to shape the CCE. The increase in electrical conductivity with reinforcement of copper strip to AC electrode attributed the improvement in the surface properties of the electrode, which provides more driving force for adsorption [23–25].

2.4. Preparation of stock solution

Eosin-Y is the dye substance obtained from Sisco Research Laboratories Pvt. Ltd. (Maharashtra, India). 0.5 g of dye was taken in 500 mL of distilled water; concentration of the dye solution was 1,000 mg L^{-1} [26]. Eosin-Y dye solution showed

Table 1
Comparison efficiency of different adsorbent prepared with phosphoric acid activation

Reacting agent	Adsorbent used	Adsorption efficiency (%)	References
H_3PO_4	Bamboo stem	92.70	[15]
	Persea americana	92.00	[16]
	Pomegranate peel	85.67	[17]
	Peach stones	70.89	[18]
	Grape seeds	65.34	[19]
	Bael shell	96.57	Present study

intense absorption peak in the visible region at 516 nm. Hence, the calibration curve for quantitative analysis was obtained at 516 nm for eosin-Y dye concentration range of 0–6 mg L^{-1}.

2.5. Determination of point of zero charge (pH_{PZC})

The point of zero charge (pH_{PZC}) of AC made from bael fruit shell was determined by solid addition method. The net charge of the adsorbent surface was zero at pH_{PZC}. Batch equilibrium method was used for the determination of pH_{PZC}. To each of the Erlenmeyer's flask, 0.5 g of bael shell adsorbent powder and 40 mL of KNO_3 (0.1 M) solution were added, and the initial pH (pH_i) was adjusted in the range from 2 to 10 by adding few drops of 0.5 M NaOH and 0.5 M HCl solution. Then each flask was sealed tightly and kept in the incubator shaker for 24 h at room temperature, and the final pH (pH_f) of the solution was noted. The difference between the pH_i and pH_f values (ΔpH) vs. pH_i was plotted as shown in Fig. 1. The pH_{PZC} of the bael shell was determined by using the point of intersection of the resulting curve at which ΔpH was zero [27,28].

2.6. Experimental procedure

Commonly electrosorption is expounded as polarization potential persuade occurrence where it took place on the surface of the charged electrodes. The batch-mode electrosorption experiments were carried out using a potentiostat (Model RPS 3002; Bee Technologies, Bangkok, Thailand) with two electrodes, as shown in Fig. 2. The working electrode used in these experiments were fabricated electrodes (ACE and CCE), and copper was used as a counter electrode. The electrochemical cell (ECC) was connected to the power supply with a voltage varying meter. In this study, experiments were conducted with 200 mL of 100 mg L^{-1} synthetic eosin-Y dye solution. The electrosorption experiments were carried out at various positive bias potentials ranging from 5 to 45 V. The negatively charged anionic dyes were scattered in the solution, and it moves toward the positively charged electrode, and the dyes were settled on the surface of ACE and CCE [11]. The durations of the electrosorption experiment were varied to study the time effect. The treated solutions were taken out from ECC at a respective time interval, and the solution was filtrated using Whatman filter paper (90 mm Ø). Further, 5 mL sample was centrifuged at 12,000 rpm for 20 min, and the solution was analyzed with the UV-visible spectrophotometric method at a wavelength of 516 nm for the presence of eosin-Y dye. The percentage dye removal (% *R*) was calculated using Eq. (1):

$$\% R = \frac{C_i - C_o}{C_i} \times 100 \quad (1)$$

where C_i and C_o are dye concentrations before and after electrosorption, respectively. The percentage dye removal at different experimental conditions were compared for both fabricated electrodes (ACE and CCE) [12,29,30].

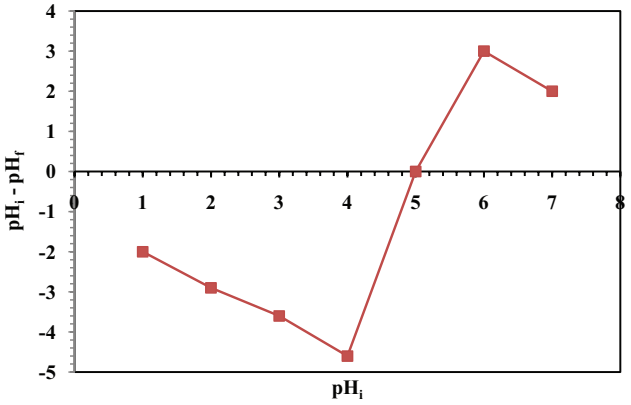

Fig. 1. Point of zero charge of BS.

3. Results and discussions

3.1. Scanning electron microscope and energy-dispersive X-ray spectroscopy characterization

Scanning electron microscope (SEM) image of BS before activation showed that the surface was plain without any pores on it, due to charged anionic dye that were not able to adsorb onto the surface of BS as illustrated in Fig. 3(a) before activation, where as Fig. 3(b) represents the changes (development of pores) on the surface of the BS after H_3PO_4 activation, phosphoric acid changed or modified the surface chemistry

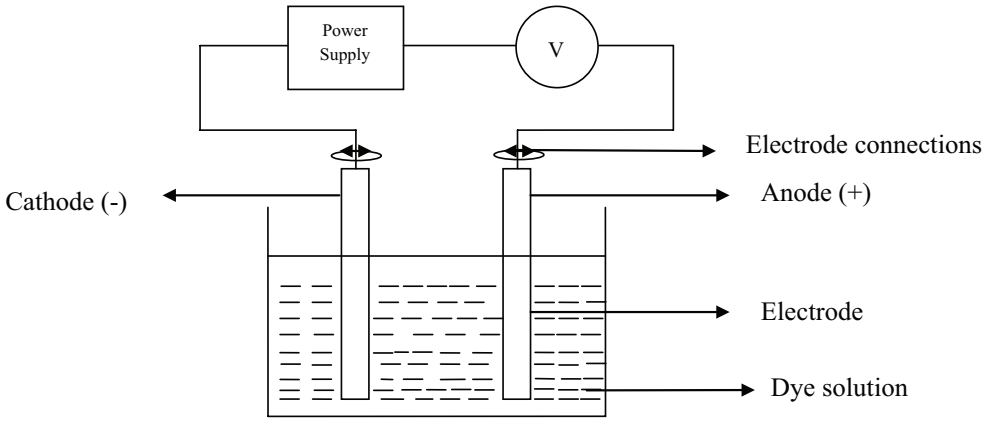

Fig. 2. Experimental setup for electrosorption.

of adsorbent due to the formation of acidic oxygen-contained complexes by strong oxidization. Also, increase in temperature resulted in weight losses and release of volatile products due to intensifying dehydration and elimination reactions; finally, these cavities formed as active pores on BS. Hence, charged anionic dyes were easily adsorbed on the surface of activated BS. From Fig. 3(c), it is seen that after electrosorption the charged anionic dyes are segmented in the surface of pores in ACE. It is neatly observed that adsorbed anionic dyes are the newly formed layer on the heterogeneous surface and some may be inside the pores of ACE [13].

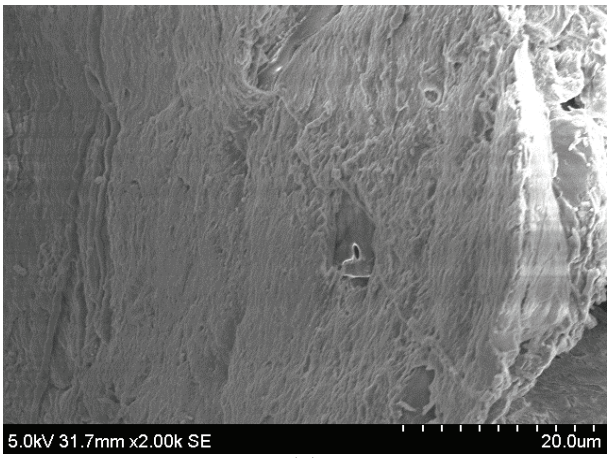

(a)

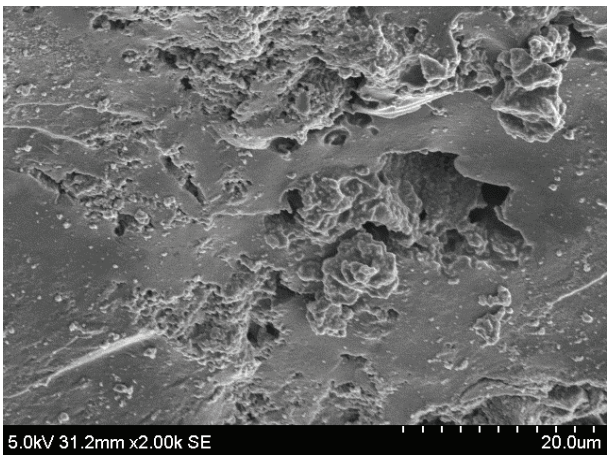

(b)

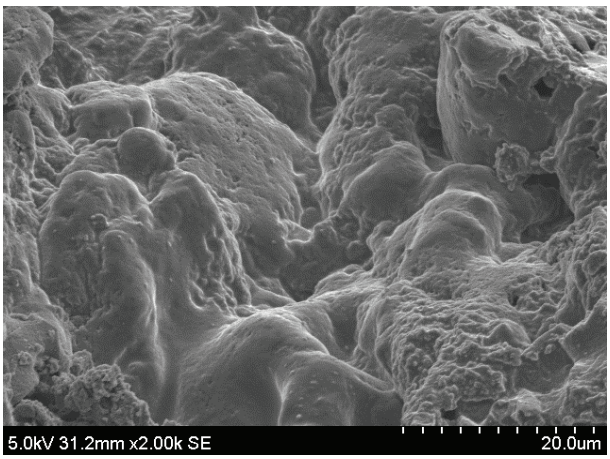

(c)

Fig. 3. SEM morphology: (a) BS before activation, (b) BS after activation and (c) ACE after electrosorption.

3.2. Energy-dispersive X-ray spectroscopy analysis

The energy-dispersive X-ray spectroscopy (EDS) spectra of BS before and after dye electrosorption were illustrated in Figs. 4(a) and (b). Many researcher's investigations reported that natural adsorbents carry large oxygen surface groups like acidic character (carboxylic), non-acidic (carbonyl) anhydride and phenol group [22]. It was noted from Fig. 4(a) that the adsorbent is having the carbon, oxygen and phosphorous elements on its surface before interaction with ions, and in Fig. 4(b), new bromine peak was observed along with the surface bearing groups of carbon, oxygen and phosphorous, which confirmed the adsorption of eosin-Y dye on the surface of the ACE [31].

3.3. Fourier transforms infrared analysis

Fig. 5 shows that the Fourier transforms infrared (FT-IR) spectra of ACE before and after eosin-Y dye adsorption. The FT-IR spectra were recorded to obtain the information regarding wave number changes (peak shifting) on the

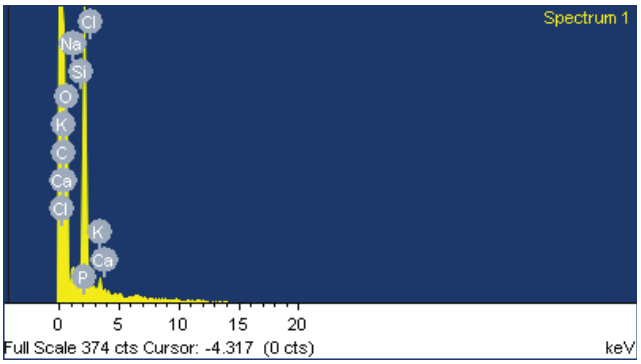

(a)

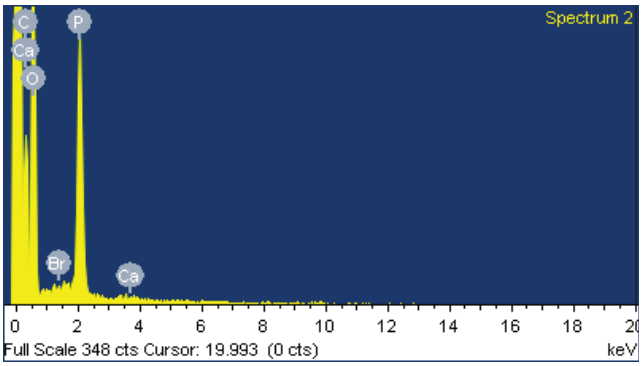

(b)

Fig. 4. EDS analysis: (a) BS before dye electrosorption and (b) BS after dye electrosorption.

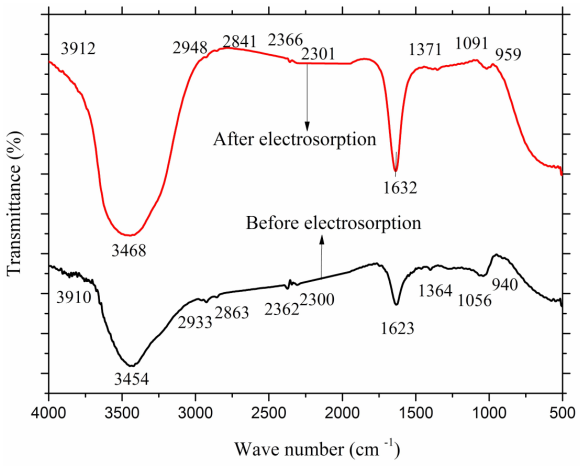

Fig. 5. FT-IR spectra of eosin-Y dye before and after electrosorption treatment.

functional groups in the range of 500–4,000 cm^{-1}. The FT-IR spectra before electrosorption showed a particular peak at corresponding wave numbers of 3,910.12, 3,454.06, 2,933.61, 2,863, 2,362.56, 2,300.23, 1,623, 1,364.56, 1,056.28 and 940 cm^{-1}, which specified the appearance of NH, C=C, OH, C–H, CO and C–Cl or C–Br functional groups, respectively. However, after eosin-Y dye adsorption, the peaks had slight variations at the wave numbers of 3,912.42, 3,468.24, 2,943.644, 2,841.64, 2,366.15, 2,301.11, 1,632.41, 1,371.89, 1,091.62 and 959 cm^{-1}. These wave numbers are acknowledging that the eosin-Y dye ions adhesion took place on the above-listed functional groups. A significant shift of C=O from 1,623 to 1,632 cm^{-1} confirms the interaction of dye molecule [32]. Further, the peak at 1,630 cm^{-1} was attributed to the amine group; it shows the lower wave number of 1,632 cm^{-1} after eosin-Y dye adsorption, which indicates the hydrogen bond formation between the O–H group of AC and N–H groups of dye molecules. Thus, the FT-IR showed the stronger probability for adsorption of eosin-Y dye ions in a batch process.

Activating agents play a critical role in surface area and porosity development. The surface area and pore size of AC adsorbent were determined by using Brunauer-Emmett-Teller surface area analyzer (Micromeritics ASAP 2020 Porosimeter). The surface area and pore volume of AC prepared from bael fruit shell by H_3PO_4 activation were 321 m^2/g and 0.323 cm^3/g, respectively, as represented in Table 2.

The removal of eosin-Y dye from aqueous solution by ACE and CCE were optimized by varying the parameters like time, electric potential and initial dye concentration.

3.4. Thermogravimetric analysis

Thermogravimetric analysis (TGA) was performed in order to evaluate the thermal stability of the BS. TGA of the raw BS was carried out by a thermogravimetric analyzer (Model-Q50, TA Instruments, New Castle, DE, USA). 10 mg of the sample was taken in a silica crucible and subjected to pyrolysis at 750°C with a heating rate of 10°C/min at N_2 atmosphere. Fig. 6 represents the two stages of thermal degradation of BS. In the first stage at 50°C–110°C, around 8% of weight loss occurred due to moisture content dried off

Table 2
Surface area of the bael shell adsorbent by different activation agents

Activation agent	Surface area (m^2/g)	Pore volume (cm^3/g)
NaCl	107	0.216
HCl	128	0.218
NaOH	176	0.289
H_2SO_4	256	0.304
KOH	289	0.311
H_3PO_4	321[a]	0.323[a]

[a]Compared with other activating agent H_3PO_4 gives higher surface area and pore volume.

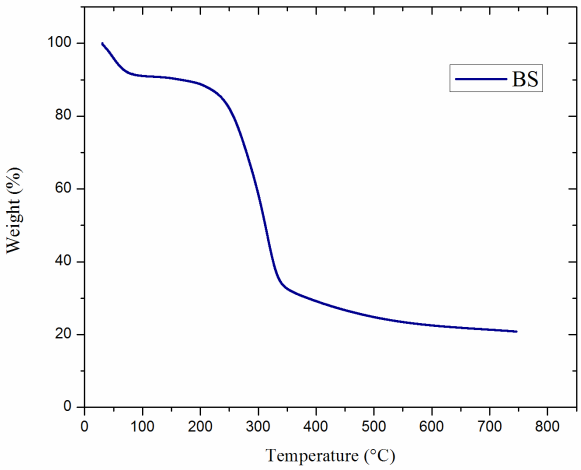

Fig. 6. Thermogravimetric analysis curve of the BS.

from the material. The second stage of thermal degradation occurred at 340°C with a weight loss of 63%, which is six times higher than the weight loss occurred in the first stage. In the temperature range of 110°C–340°C, huge weight loss was taken place due to the vaporization of organic components present in the BS like cellulose, lignin, hemocellulose, etc. When the sample was heated above 340°C, the TGA curve flattens with no change in weight thereafter. The TGA analysis indicates the better thermal stability of BS.

3.5. Effect of time

Fig. 7 represents the contact time behavior of dye solution on ACE and CCE. The graph was drawn between contact time and percentage dye removal on ACE and CCE. The initial dye concentration of 100 mg L^{-1} and 5 V of bias potential were maintained constant, and time was varied. It was observed that contact time was increased from 15 to 120 min and the percentage removal was increased from 5.72% to 39.32%, respectively, for ACE. Similar trend was noticed for CCE also; percentage dye removal increased from 10.68% to 95.44%, respectively. In the initial intervals of time, the percentage removal is low, because the reaction time between dyes (eosin-Y), ACE and CCE is less. From the results, it was observed that CCE provides better removal efficiency than ACE because inclusion of copper metallic strip on to AC had a better effect on conductivity.

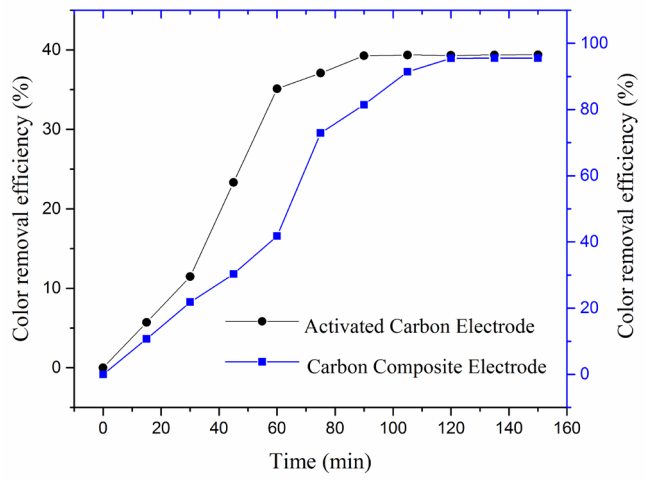

Fig. 7. The efficiency of eosin-Y removal under optimum conditions (dye concentration: 100 mg L^{-1}, bias potential: 5 V).

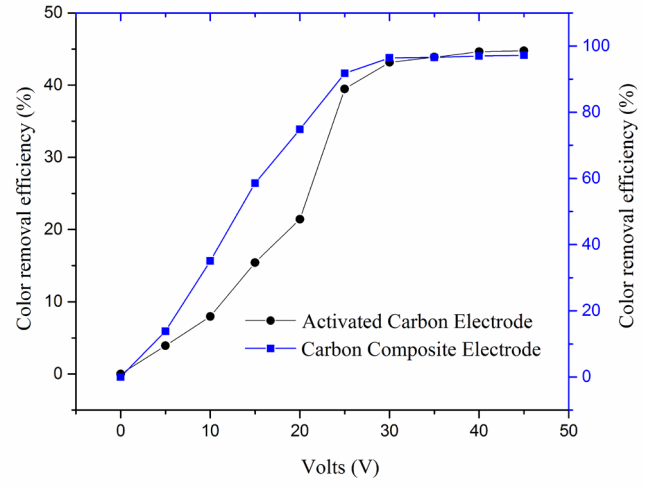

Fig. 8. The efficiency of eosin-Y removal under optimum conditions (dye concentration: 100 mg L^{-1}, time: 30 min).

3.6. Effect of voltage

Fig. 8 represents the voltage behavior of dye solution on ACE and CCE. The potential parameter was varied, by maintaining initial dye concentration and time at a constant value of 100 mg L^{-1} and 30 min, respectively. From the results, it is clear that when potential increases from 5 to 30 V, the percentage color removal increases from 3.92% to 43.16%, respectively, for ACE, likewise for CCE percentage color removal increases from 13.84% to 96.43%, respectively. Beyond 30 V, there was no noticeable change in percentage color removal. Generally, in all electrochemical processes, energy consumption increases as applied potential increases along with percentage color removal. CCE resulted in high percentage color removal compared with ACE.

3.7. Effect of initial dye concentration

Fig. 9 shows that the effect of initial dye concentration on ACE and CCE. It can be seen that in ACE and CCE electrosorption performance decreases with the increase in initial dye concentration, and obtained saturation after equilibrium time. The percentage removal shows that with an increase in the initial concentration of dyes, the percentage removal decreased from 29.92% to 1.56% (eosin-Y on to ACE) and 71.36% to 24.96% (eosin-Y on to CCE) for the dye concentration from 25 to 200 mg L^{-1}; this depends on the pores available on surface of ACE and CCE and bond formation between dyes and ACE and CCE.

3.8. Comparison between ACE and CCE with commercial electrode

Figs. 10(a)–(c) show the effect of time, voltage and initial dye concentration behavior on dye removal. Electrode prepared from commercial AC is known as commercial electrode, the physical properties such as pore volume (0.981 cm^3/g), surface area (1,057.17 m^2/g) and electrical

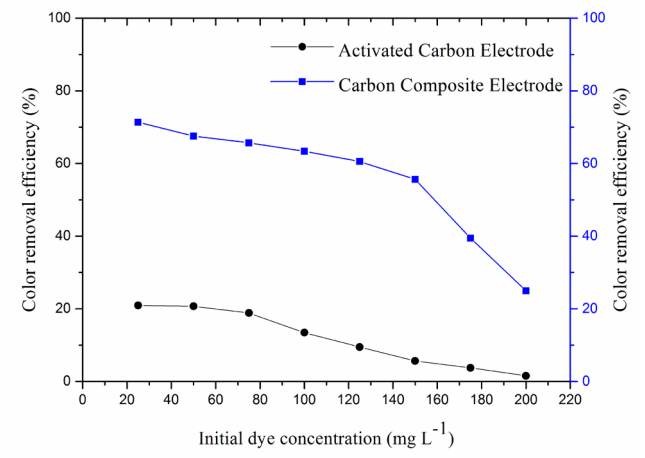

Fig. 9. The efficiency of eosin-Y removal under optimum conditions (bias potential: 5 V, time: 30 min).

conductivity (600 mS/cm) are good compared with the fabricated electrode ACE (8.3 mS/cm). The electrical conductivity of CCE is 10 times higher than commercial electrode due to the inclusion of copper metal strip. From the graphs, it is noticed that CCE removed eosin-Y dye to a higher rate at a defined time, voltage and initial dye concentration compared with ACE.

4. Adsorption isotherms

Adsorption isotherms, known as equilibrium data, are the fundamental requirements for the design of adsorption systems. Normally, adsorption process was controlled by the interaction between the two systems, such as adsorbent surface and adsorbed species. The chemical bonding, hydrogen bonding, hydrophobic and van der Waals forces are maybe the reason to take place reaction between the adsorbent and adsorbate. The equilibrium data for the batch

adsorption of eosin-Y onto ACE was analyzed using three isotherm models to know the maximum adsorption capacity of electrosorption process. Most frequently used two-parameter models are Langmuir, Freundlich and Jovanovic isotherm.

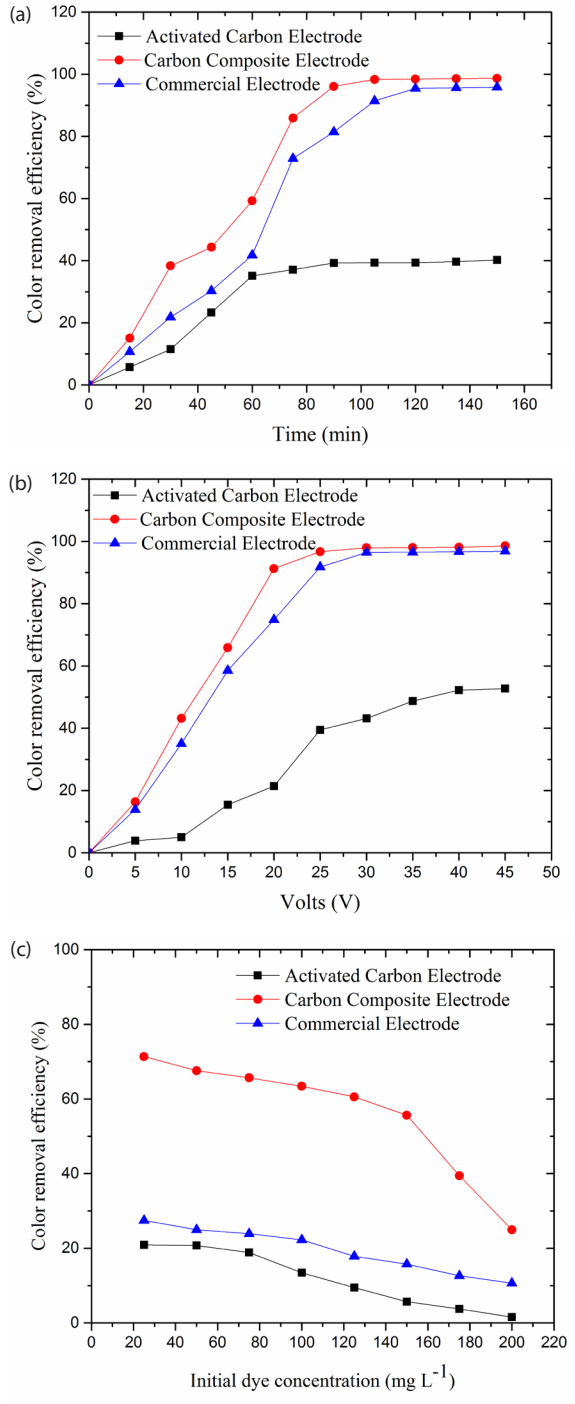

Fig. 10. (a) The effect of time on eosin-Y removal (dye concentration: 100 mg L^{-1}, bias potential: 5 V); (b) The effect of bias potential on eosin-Y removal (dye concentration: 100 mg L^{-1}, time: 30 min); (c). The effect of initial dye concentration on eosin-Y removal (bias potential: 5 V, time: 30 min).

4.1. Langmuir isotherm

The Langmuir isotherm has a theoretical basis and the equation was derived by assuming that there are only a fixed number of active sites available for adsorption, that only a monolayer is formed, and that the adsorption is reversible and reaches the equilibrium condition. The linearized form of Langmuir adsorption isotherm equation is as follows:

$$\frac{C_e}{q_e} = \frac{1}{Q_o b_L} + \frac{C_e}{Q_o} \quad (2)$$

The Langmuir constants Q_o (mg/g) and b_L (L/mg) are calculated by plotting C_e/q_e vs. C_e. The isotherm parameters and correlation coefficient are shown in Table 3.

4.2. Freundlich isotherm

The Freundlich isotherm model equation describes adsorption with possible multilayer on a highly heterogeneous surface consisting of non-identical and energetically non-uniform sites [33,34]. The linearized form of Freundlich adsorption isotherm equation is as follows:

$$\log q_e = \log K_F + \frac{1}{n_F} \log C_e \quad (3)$$

The Freundlich constants K_F ($mg^{1-1/n}$ $L^{1/n}$ g^{-1}) and n_F were calculated from the slope and intercept of the linear plot ($\log q_e$ vs. $\log C_e$. n_F value greater than one confirms adsorption is favorable. Also based on correlation coefficients (R^2 = 0.923), Freundlich isotherm found to fit well compared with other isotherms, which indicates that the eosin-Y electroadsorption on ACE and CCE was heterogeneous in nature. The linear form of Freundlich adsorption isotherm equation for eosin-Y electrosorption is illustrated in Fig. 11. The isotherm parameters were listed in Table 3. The actual amount of eosin-Y uptake increased with increased initial dye concentration, as illustrated in Fig. 12. This is due to increase in the driving force of the concentration gradient, with the increase of the initial dye concentration.

4.3. Jovanovic isotherm

The Jovanovic isotherm adsorption is essentially same like Langmuir isotherm; same kind of approximation leads to the

Table 3
Isotherm model constant for eosin–Y adsorption on to bael shell

Isotherm models	Parameters	Values
Langmuir	Q_o (mg/g)	47.61
	b_L (L/mg)	0.023
	R^2	0.734
Freundlich	K_F ($mg^{1-1/n}$ $L^{1/n}$ g^{-1})	1.976
	n_F	1.485
	R^2	0.923
Jovanovic	q_{mj} (mg/g)	3.14×10^{-58}
	K_j (L/mg)	-1.37×10^{59}
	R^2	0.891

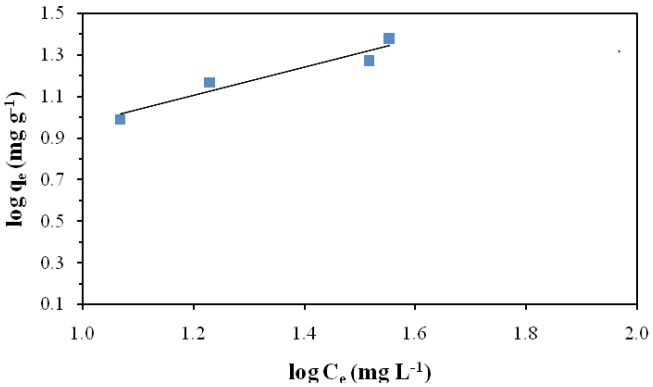

Fig. 11. Plot of Freundlich isotherms for the electrosorption of eosin-Y onto BS.

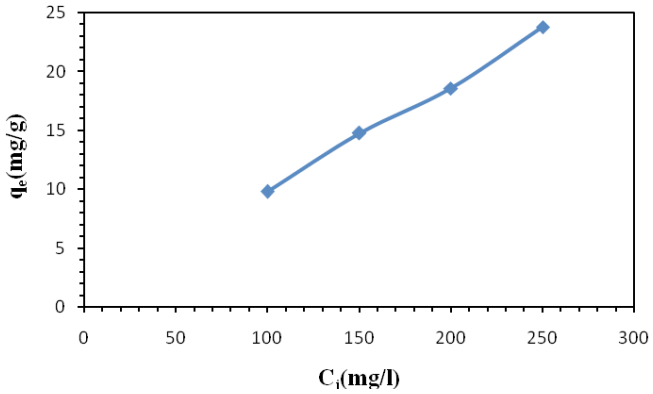

Fig. 12. Electrosorption capacity of BS at different initial eosin-Y concentration.

monolayer adsorption without lateral interactions. The model considers the few possibilities of mechanical contacts between the adsorption and desorbing molecules. The linear form of Jovanovic adsorption isotherm equation is as follows:

$$\log q_e = q_{mj} - q_{mj} \cdot e^{K_j C_e} \tag{4}$$

where q_{mj} (mg/g) and K_j (L/mg) are the adsorption capacity and Jovanovic isotherm constants, respectively. The correlation coefficient (R^2), K_j and q_{mj} were calculated from the plot of logq_e vs. C_e and listed in the Table 3.

5. Kinetic studies

Adsorption kinetic study is a major factor in determining the efficacy of adsorption. The analysis over the adsorption kinetics is a vital stage for designing the batch adsorption systems. The kinetics of eosin-Y dye adsorption was analyzed using pseudo-first-order, pseudo-second-order and intraparticle diffusion models.

5.1. Pseudo-first-order model

The pseudo-first-order rate equation of Lagergren is as follows:

$$\log\left(q_e - q_t\right) = \log q_e - \frac{k_1}{2.303} t \tag{5}$$

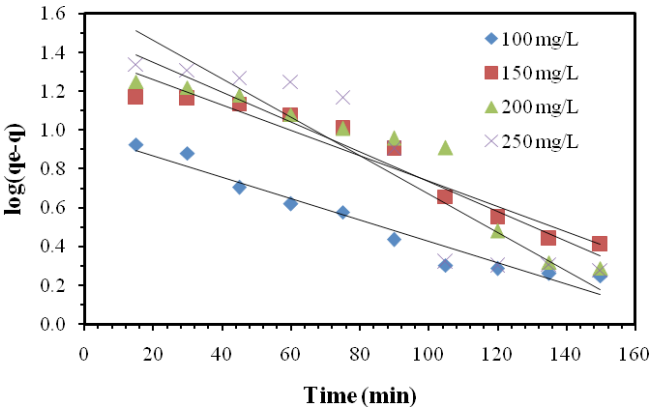

Fig. 13. Pseudo-first-order kinetics plot for electrosorption of eosin-Y by BS.

where q_e and q_t are the amount of eosin-Y adsorbed (mg/g) at equilibrium time and at any time t. k_1 (min) is the pseudo-first-order rate constant. The pseudo-first-order considers the rate of occupation of adsorption sites to be proportional to the number of unaccommodated sites. The constant values of pseudo-first-order were calculated from the graph log($q_e - q$) vs. t and shown in Fig. 13. The adsorption kinetics was fitted to the Lagergren law by non-linear regression using the method of least squares. The adsorption capacity of eosin-Y dye solution increased as concentrations of the solutions increased, as illustrated in Table 4. The pseudo-first-order model well fitted with the equilibrium data. The calculated adsorption capacity value suggested that the pseudo-first-order model was appropriate for modeling the electrosorption of eosin-Y onto BS.

5.2. Pseudo-second-order model

The pseudo-second-order kinetic model can be expressed as follows:

$$\frac{t}{q_t} = \frac{1}{k_2 q_e^2} + \frac{t}{q_e} \tag{6}$$

where k_2 (g/mg/min) is the rate constant for pseudo-second-order model.

The constant values of pseudo-second-order were calculated from the graph t/q_t vs. t and shown in Table 4.

5.3. Intraparticle diffusion

Intraparticle diffusion model insights the mechanisms and rate-controlling steps that affect the electrosorption kinetics and represented using the following equation:

$$q_t = k_{id} t^{1/2} + C \tag{7}$$

where k_{id} is the intraparticle rate constant diffusion (mg/g/min$^{1/2}$), and C is the intercept. The plot of q_t against $t^{0.5}$ is illustrated in Fig. 14, and this kinetic model constant values were represented in Table 4. From Fig. 14, it was observed that the plots were neither linear nor passing through origin; thus, the intraparticle diffusion was not only rate-controlling step,

Table 4
Kinetic model rate constants for eosin-Y adsorption onto bael shell

Kinetic model parameter	Initial eosin-Y dye concentration (mg/L)			
	100	150	200	250
Pseudo-first-order				
K_1 (min^{-1})	0.0299	0.0230	0.018	0.018
q_e (mg/g)	23.06	37.32	36.30	42.07
R^2	0.969	0.909	0.850	0.846
Pseudo-second-order				
K_2 (g/mg/min)	0.594	0.010	9.93×10^{-4}	8.246×10^{-5}
q_e (mg/g)	0.165	0.850	6.329	34.48
R^2	0.305	0.386	0.600	0.535
Intraparticle diffusion				
K_{id} (mg/g/min$^{1/2}$)	1.574	1.949	2.18	2.84
C (mg/g)	–7.039	–10.53	–10.06	–12.92
R^2	0.932	0.847	0.928	0.850

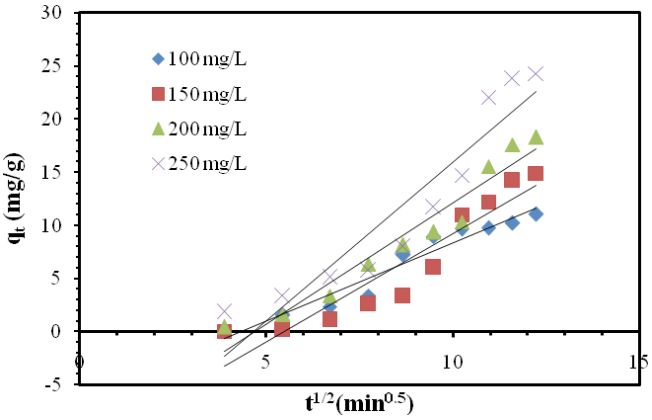

Fig. 14. Intraparticle diffusion model for the removal of eosin-Y by BS.

and also the film diffusion might be involved in the electrosorption of eosin-Y dye by BS [22,35].

5.4. Energy consumption

The foremost important parameters in the electrosorption treatment technologies are energy consumption. The major operating cost is calculated with the electrical energy consumption during the electrochemical process. The increase in applied potential increased the specific energy consumption for the removal of eosin-Y dye from aqueous solution. At minimum potential (5 V) and contact time (30 min), around 63.4% color removal was observed for initial dye concentration of 100 mg L^{-1}.

6. Conclusion

The present study addressed about the preparation of AC, ACE and CCE electrodes for the application of decolorization of eosin-Y dye effluent. It confirms that fabricated electrodes enhanced the color removal efficiency were compared with raw BS. The BS adsorbent achieved higher surface area (321 m^2/g) with phosphoric acid activation. The maximum removal efficiency (97.12%) was obtained for the color removal with an optimum operating conditions 100 mg L^{-1} of initial dye concentration, 30 min of contact time and 30 V of applied potential. The characterization techniques (FT-IR, SEM, EDS and TGA) provide the physicochemical properties of BS, ACE and CCE. The batch electrosorption equilibrium studies fitted well for Freundlich isotherm model and pseudo-first-order kinetic model, respectively. Freundlich isotherm model represents the adsorption of ACE and CCE surface, which is vigorously non-uniform. Hence, the low-cost, abundantly available BS would be used as a competent, economical and eco-friendly bioadsorbent for the removal of dyes from textile industry effluents by electrosorption process.

Acknowledgment

The financial support of National Institute of Technology Calicut, India, and KSCSTE, Thiruvananthapuram, Kerala (Project No. 1: 71/SPS 57/2016/KSCSTE, Project No. 2: ETP/16/2015/KSCSTE) is gratefully acknowledged.

References

[1] M. Caldera Villalobos, A.A. Pelaez Cid, A.M. Herrera Gonzalez, Removal of textile dyes and metallic ions using polyelectrolytes and macroelectrolytes containing sulfonic acid groups, J. Environ. Manage., 177 (2016) 65–73.
[2] R.V. Khandare, S.P. Govindwar, Phytoremediation of textile dyes and effluents: current scenario and future prospects, Biotechnol. Adv., 33 (2015) 1697–1714.
[3] Y. Han, X. Quan, S. Chen, H. Zhao, C. Cui, Y. Zhao, Electrochemically enhanced adsorption of phenol on activated carbon fibers in basic aqueous solution, J. Colloid Interface Sci., 299 (2006) 766–771.
[4] H. Li, Y. Gao, L. Pan, Y. Zhang, Y. Chen, Z. Sun, Electrosorptive desalination by carbon nanotubes and nanofibres electrodes and ion-exchange membranes, Water Res., 42 (2008) 4923–4928.
[5] Y. Oren, Capacitive deionization (CDI) for desalination and water treatment – past, present and future (a review), Desalination, 228 (2008) 10–29.
[6] A. Ban, H. Schafer, H. Wendt, Fundamentals of electrosorption on activated carbon for wastewater treatment of industrial effluents, J. Electrochem., 28 (1998) 227–236.
[7] E. Bayram, E. Ayranci, Electrosorption based waste water treatment system using activated carbon cloth electrode: electrosorption of benzoic acid from a flow-through electrolytic cell, Sep. Purif. Technol., 86 (2012) 113–118.
[8] B.B. Arnold, G.W. Murphy, Studies on the electrochemistry of carbon and chemically-modified carbon surfaces, J. Phys. Chem., 65 (1961) 135–138.
[9] A.M. Johnson, J. Newman, Desalting by means of porous carbon electrodes, J. Electrochem. Soc., 118 (1971) 510–517.
[10] Y. Oren, A. Soffer, Water desalting by means of electrochemical parametric pumping: I. The equilibrium properties of a batch unit cell, J. Appl. Electrochem., 13 (1983) 473–487.
[11] A. Pirkarami, M.E. Olya, N. Yousefi Limaee, Decolorization of azo dyes by photo electro adsorption process using polyaniline coated electrode, Prog. Org. Coat., 76 (2013) 682–688.
[12] A.S. Koparal, Y. Yavuz, U. Bakir Ogutveren, Electroadsorption of acilan blau dye from textile effluents by using activated carbon-perlite mixtures, Water Environ. Res., 74 (2002) 521–525.
[13] J. Anandkumar, B. Mandal, Removal of Cr(VI) from aqueous solution using bael fruit (*Aegle marmelos correa*) shell as an adsorbent, J. Hazard. Mater., 168 (2009) 633–640.

[14] L. Zou, G. Morris, D. Qi, Using activated carbon electrode in electrosorptive deionisation of brackish water, Desalination, 225 (2008) 329–340.
[15] Y. Rajesh, M. Pujari, R. Uppaluri, Equilibrium and kinetic studies of Ni(II) adsorption using pineapple and bamboo stem based adsorbents, Sep. Sci. Technol., 49 (2014) 533–544.
[16] A. Regti, M.R. Laamari, S.-E. Stiriba, M. El Haddad, Removal of Basic Blue 41 dyes using *Persea americana*-activated carbon prepared by phosphoric acid action, Int. J. Ind. Chem., (2016). doi: 10.1007/s40090-016-0090-z.
[17] E.S.Z. El-Ashtoukhy, N.K. Amin, O. Abdelwahab, Removal of lead (II) and copper (II) from aqueous solution using pomegranate peel as a new adsorbent, Desalination, 223 (2008) 162–173.
[18] A.A. Attia, B.S. Girgis, N.A. Fathy, Removal of methylene blue by carbons derived from peach stones by H_3PO_4 activation: batch and column studies, Dyes Pigm., 76 (2008) 282–289.
[19] M. Al Bahri, L. Calvo, M.A. Gilarranz, J.J. Rodriguez, Activated carbon from grape seeds upon chemical activation with phosphoric acid: application to the adsorption of diuron from water, Chem. Eng. J., 203 (2012) 348–356.
[20] H. Sharififard, M. Soleimani, F.Z. Ashtiani, Evaluation of activated carbon and bio-polymer modified activated carbon performance for palladium and platinum removal, J. Taiwan Inst. Chem. Eng., 43 (2012) 696–703.
[21] C.H. Hou, J.F. Huang, H.R. Lin, B.Y. Wang, Preparation of activated carbon sheet electrode assisted electrosorption process, J. Taiwan Inst. Chem. Eng., 43 (2012) 473–479.
[22] E. Gonzalez-Serrano, T. Cordero, J. Rodriguez-Mirasol, L. Cotoruelo, J.J. Rodriguez, Removal of water pollutants with activated carbons prepared from H_3PO_4 activation of lignin from kraft black liquors, Water Res., 38 (2004) 3043–3050.
[23] J.H. Choi, Fabrication of a carbon electrode using activated carbon powder and application to the capacitive deionization process, Sep. Purif. Technol., 70 (2010) 362–366.
[24] L.M. Chang, X.Y. Duan, W. Liu, Preparation and electrosorption desalination performance of activated carbon electrode with titania, Desalination, 270 (2011) 285–290.
[25] Y. Kong, W. Li, Z. Wang, C. Yao, Y. Tao, Electrosorption behavior of copper ions with poly(m-phenylenediamine) paper electrode, Electrochem. Commun., 26 (2013) 59–62.
[26] Z.M. Reza Ansari, Removal of Eosin Y, an anionic dye, from aqueous solutions using conducting electroactive polymers, Iran. Polym. J., 19 (2010) 541–551.
[27] S. Rangabhashiyam, N. Selvaraju, Evaluation of the biosorption potential of a novel *Caryota urens* inflorescence waste biomass for the removal of hexavalent chromium from aqueous solutions, J. Taiwan Inst. Chem. Eng., 47 (2015) 59–70.
[28] A.M. Cardenas-Pena, J.G. Ibanez, R. Vasquez-Medrano, Determination of the point of zero charge for electrocoagulation precipitates from an iron anode, Int. J. Electrochem. Sci., 7 (2012) 6142–6153.
[29] W.L. Chou, C.T. Wang, C.P. Chang, Comparison of removal of Acid Orange 7 by electrooxidation using various anode materials, Desalination, 266 (2011) 201–207.
[30] D. Marmanis, A. Christoforidis, K. Ouzounis, K. Dermentzis, Electrochemical desalination of NaCl solutions by electrosorption on nano-porous carbon aerogel electrodes, Global NEST J., 16 (2014) 609–615.
[31] S.J. Mitchell, G. Brown, P.A. Rikvold, Dynamics of Br electrosorption on single-crystal Ag(100): a computational study, J. Electroanal. Chem., 493 (2000) 68–74.
[32] Y. Rajesh, G. Namrata, U. Ramgopal, Ni(II) adsorption characteristics of commercial activated carbon from synthetic electroless plating solutions, Desal. Wat. Treat., 57 (2015) 13807–13817.
[33] S. Bhuvaneshwari, V. Sivasubramanian, Equilibrium, kinetics, and breakthrough studies for adsorption of Cr(VI) on chitosan, Chem. Eng. Commun., 201 (2014) 834–854.
[34] O. Gercel, Removal of textile dye from aqueous solution by electrochemical method, Sep. Sci. Technol., 51 (2016) 711–717.
[35] Z. Chen, C. Song, X. Sun, H. Guo, G. Zhu, Kinetic and isotherm studies on the electrosorption of NaCl from aqueous solutions by activated carbon electrodes, Desalination, 267 (2011) 239–243.